Proceedings of the IASS 2024 Symposium
Redefining the Art of Structural Design
August 26-30, 2024, Zurich Switzerland
Philippe Block, Giulia Boller, Catherine DeWolf,
Jacqueline Pauli, Walter Kaufmann (eds.)

Nervi Puzzle: a topologically reconfigurable modular ribbed floor

Robin OVAL

Delft University of Technology, Faculty of Civil Engineering & Geosciences
Stevinweg 1, 2628 CN Delft, The Netherlands
r.oval@tudelft.nl

Abstract

Designing and building ribbed floors is a trade-off between mechanical efficiency, construction rationality, and circular reconfigurability. As opposed to a floor with constant thickness, introducing ribs is a means to improve material efficiency. Two extremes for ribbed floor systems are the waffle slab, highly simplified for construction rationality, with a higher embodied carbon, and the ribbed floors à la Pier Luigi Nervi, with a highly optimized material distribution for specific boundary conditions. Indeed, by following the stress field for material economy, and by leveraging contemporary digital fabrication technology, such ribbed floors can offer a low upfront embodied carbon. However, these customized monolithic structures do not allow disassembly, reuse, and reconfiguration to enable a circular economy of construction and later adapt to different boundary, support, and loading scenarios. This research presents a strategy for the geometrical modularization of ribbed floors that can be topologically reconfigured, using generative design of pattern topologies to form a catalogue of compatible modules. This paper outlines the design of a specific catalogue of modules; a bitmap description of the module configurations; several strategies for the optimization of these configurations; and a case study to assess the potential of such a modular structural system. Future research includes deeper structural optimization, and system materialization, particularly reversible joint design.

Keywords: structural design, computational design, generative design, structural optimization, grammar, topology, patterns, grillage, modularity, circular economy.

1. Introduction

Ribbed surface structures allow for material-minimum systems, as exemplified by Pier Luigi Nervi's spanning structures, particularly building floors [1]. The theoretically optimal structure is achieved with a rib pattern that follows the principal stress directions. However, these patterns lack modularity and require mass customization when the support conditions differ from a strict repetition of the boundary conditions, as shown in Figures 1a and 1b. This increases their embodied carbon due to an uneconomical buildability without mass-customization fabrication technology. On the contrary, a waffle slab with its orthogonal layout of ribs allows for construction rationalisation thanks to modularity, as shown in Figure 1c, but highly deviates from the principal stress directions, inducing a lower structural efficiency.

Modularity offers a trade-off between mass production of a single module and mass customization of every element. Modularity enables the reuse of the components, the formwork for fabrication, and the structure to expand its lifespan beyond the end-of-life of the building in the context of a circular economy of construction.

Can we design modular ribbed floors that are efficient, buildable, and circular? This research explores the design of a poly-module ribbed floor system based on a catalogue of topologically reconfigurable modules. This paper presents the design of such a specific catalogue of modules, whose (re)configurations can be encoded as a bitmap for structural optimization, as demonstrated on a case study.

Figure 1. Ribbed building floors: (a) Pier Luigi Nervi's Gatti Wool Factory in Rome, Italy [1], (b) Hans-Dieter Hecker's Lecture Hall of the Zoology Department in Freiburg, Germany [2], and (c) Holedeck's modular waffle floor system [3].

2. Module catalogue design

The design of a catalogue of modules must strike a balance between providing configurations with a maximum mechanical efficiency for the relevant range of applications and requiring a minimum number of modules to produce and manage.

The catalogue presented in this paper consists of six modules generated with the aim to obtain different combinations and configurations of grid and polar patterns, as featured in the floors with ribs following the principal stress directions in Figure 1. This catalogue is tailored for building layouts based on grids with a spacing of 2 m.

2.1. Module tessellation

The modules have a square boundary, to tessellate the plane, with an edge length of 2 m. Each module is subdivided into 4, to obtain a constant spacing of 50 cm between ribs at the interface between modules to ensure geometrical compatibility.

2.2. Rib patterns

The bi-directional ribs are represented by quad-mesh patterns, offering both grid- and pole-like areas. A catalogue of 6 modules is proposed, based on all the combinations of poles located at the corners of a square module. Choosing any combination of the four corners to position poles yields:

$$\sum_{i=0}^{4} \binom{4}{i} = 2^4 = 16 \tag{1}$$

possibilities, which correspond to all the orientations of the modules.

This number reduces to $N = 6$ when considering the modules that must be unique under any of the $g = 4$ admissible rotations, 0, $\pi/2$, π, and $3\pi/2$, using Pólya-Burnside counting [4]. When writing G^X as the ensemble of modules left invariant by rotation X, we obtain:

$$N = \frac{1}{g}\left(|G^0| + \left|G^{\pi/2}\right| + |G^{\pi}| + \left|G^{3\pi/2}\right|\right) = \frac{1}{4}(16 + 2 + 4 + 2) = 6 \tag{2}$$

as the rotations by 0, $\pi/2$, π, and $3\pi/2$ leave 16, 2, 4, and 2 modules invariant, respectively.

The modules are labelled with a sequence of four binaries specifying the absence (0) or the presence (1) of a pole at the module corner, starting at the top left and going clockwise. For instance, label 0110 means the presence of poles at the top right and bottom right corners, and only there.

The topology of the patterns is produced using feature-based topology finding [5] and a unique geometry is obtained for each of them after Laplacian smoothing with 100 iterations and 0.5 damping. Figure 2 shows the 6 unique modules with their 16 different orientations and their binary sequence labels.

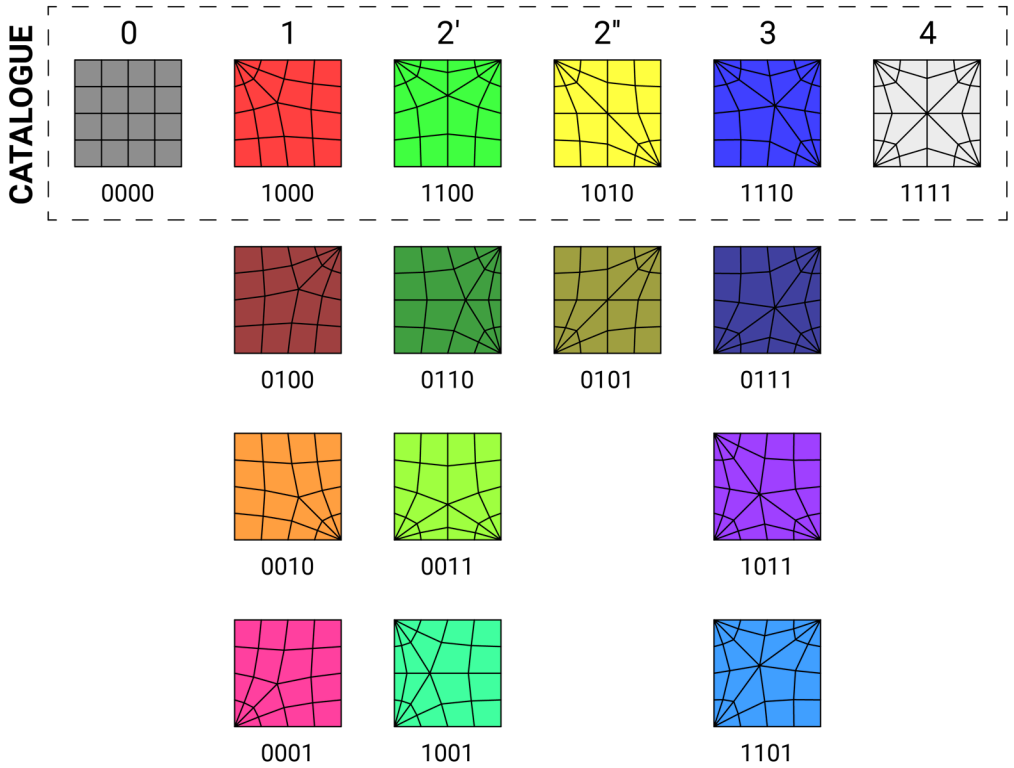

Figure 2. The 6 unique modules of the catalogue with their 16 different orientations and their binary sequence labels.

2.3. Rib dimensions

The ribs have constant height and width throughout all the modules, for compatibility at their interface.

In a more complete catalogue, the modules could be based on different tessellations, consider different base module edge length, include fractions of it, provide different densities, process geometry differently, offer different rib heights and widths, be made of different materials, and even propose other patterns. Enriching the catalogue with more modules comes at a production and management cost, and a larger configuration space to explore. Any increase in such complexity should be justified by a potential contribution in structural efficiency and reduced upfront embodied carbon.

3. Module configuration search

The design problem is encoded as a bitmap, where each pixel is allocated a module. The size of the design space is counted as the number of unique possible configurations. For a bitmap of p pixels without symmetry and m modules including orientations, the problem has a size of m^p. With a catalogue of 16 modules including their unique orientations, 10^{12} combinations are possible for a simple 3×3 grid. For a building floor area of 400 m^2 to cover with 100 of these 2 m $\times$ 2 m modules, 10^{120} combinations exist, for instance. This combinatorial problem becomes quickly intractable, therefore fast means for generating efficient module configurations are necessary.

3.1. Heuristic methods

3.1.1. Support conditions

The first method is based on the initial heuristic used to generate the catalogue, which is derived from the flow of forces towards the column and wall supports seen in Figure 1. This heuristic positions modules with poles around columns and walls, to have the ribs attracted to them, as illustrated in Figure 3. This method is automated, needing only the boundary conditions, and does not require any structural analysis.

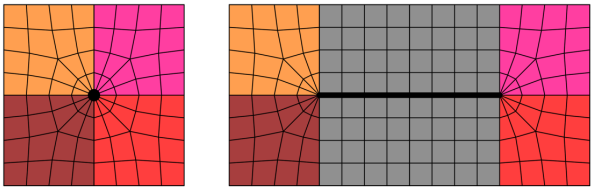

Figure 3. Heuristic positioning of module poles at the columns in all directions and at the wall extremities in the outward direction.

3.1.2 Stress field

The second method relies on an initial structural analysis of a continuous plate with the same boundary conditions and computing the stress field. At each pixel $\boldsymbol{P}$, the module $\boldsymbol{M}$ that best fits the local stress field based on a score is selected. This ad hoc fitness score is assessed as a weighted sum over all the vertices of the average smallest angle between each edge and the local cross field to find the best module $\boldsymbol{M_P}$:

$$M_P = \underset{M}{\operatorname{argmin}} \sum_{v \in V} \frac{A_v}{A} \frac{1}{|E_v|} \sum_{e \in E_v} \theta(e, s_v) \tag{3}$$

where A is the area of the module, A_v the tributary area of vertex v, V the set of vertices, E_v the set of edges connected to vertex v, and $\theta(e, s_v)$ the smallest angle between the vector of edge e and the four directions of the stress cross field s_v at vertex v. Figure 4 illustrates these different geometrical objects for a specific vertex. This method requires a single structural analysis as well as providing $m \cdot p$ scores for the m modules at the p pixels.

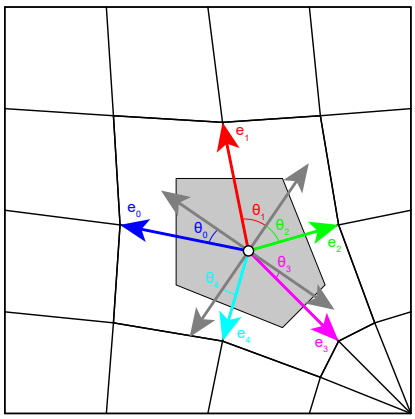

Figure 4. Fitness score evaluation between a module mesh and the local stress field at a pixel based on vector alignment. For a vertex represented by the white dot, the vertex tributary area is shown in light grey, the local cross field in dark grey, and the edge vectors e_i with their smallest angle with the cross field θ_i in different colours.

3.2. Numerical optimization

The bitmap encoding of the problem makes modular configuration search suitable for discrete numerical optimization. This approach includes stochastic methods like evolutionary algorithm and simulated annealing, implemented in Galapagos for Grasshopper [6]. These methods require multiple structural analyses of the grillage structures to search for an optimum based on a performance objective to minimize.

4. Case study

A single case study, including several interesting features, is used to test the catalogue and compare the search methods. Such work should be performed on a range of relevant design scenarios for benchmarking and designing an efficient catalogue.

4.1. Design problem description

The building floor plan shown in Figure 5 is considered. It consists of an L-shape boundary with a square hole (thin dark lines), supported by a wall (thick line) and four columns (thick dots). The bitmap (dashed grey lines) has 13 pixels and therefore $16^{13} \approx 10^{15}$ possible configurations. The stress field (red and blue crosses) under uniform loading of the equivalent continuous plate structure is used for heuristic search.

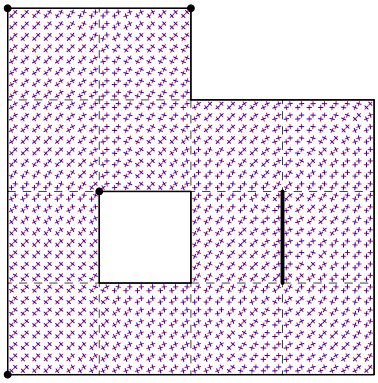

Figure 5. Building floor case study with a wall (thick line) and four column (thick dots) supports, a 13-pixel bitmap to fill with 2 m × 2 m modules (dashed grey lines), and stress field information (red and blue crosses).

The module configurations are analysed as a grillage, using linear elastic theory, implemented in Karamba for Grasshopper [7]. The loads considered are the self-weight G and a symmetrical uniform loading Q of 5 kN/m^2. A C30/37 concrete material is selected, with a density of 25 kN/m^3, an initial elastic stiffness of 33 GPa, and a Poisson's ratio of 0.2. The beams all have a height of 20 cm. The width is tuned so that each design has the same mass of 1.4 t for this case study. This mass is obtained from the orthogonal grid design with a width of 10 cm. All intra- and inter-module connections are supposed rigid. The elastic energy is used as a metric to minimize, heuristically or numerically, for comparing the structural performance of the different design configurations found.

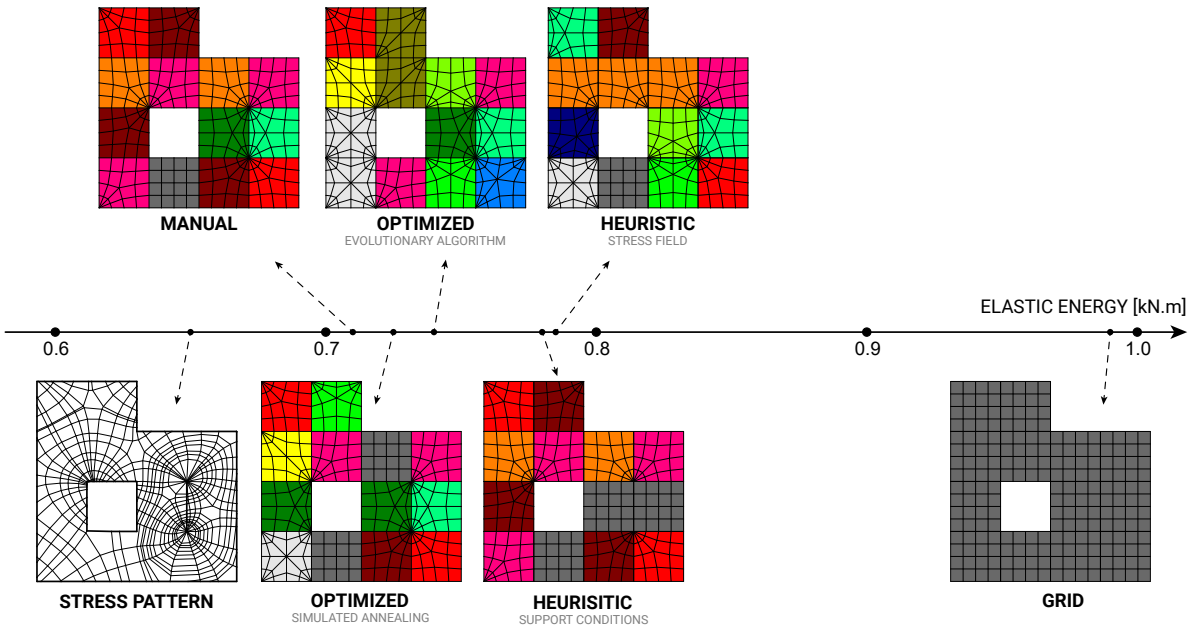

Figure 6. Single-module, poly-module, and non-modular ribbed floors sorted based on their elastic energy.

4.2. Single load case optimization

First, the single load combination $G + Q$ is considered. The four designs automatically found with the heuristic and optimization methods are shown in Figure 6, sorted by performance in terms of elastic energy, with numerical values in Table 1, with a color gradient to highlight the best designs in green and the worst ones in red, for visualization. The results for the regular grid of the waffle slab, a non-modular stress pattern, and a modular design obtained manually but informed by other design configurations are also included. The single-module waffle slab has the worst performance and is used as a benchmark to compare improvements in terms of elastic energy obtained with the proposed poly-module system. The two heuristic designs offer a reduction of 21%. The two designs found with stochastic optimization achieved a slightly higher reduction of 25-27%. The non-modular pattern based on the stress lines produced from the integration of the stress field resulted in the highest reduction of 34%. Considering the results obtained through stochastic optimization and the stress lines for this specific building floor, a modular design was derived manually by adding a heuristic based on the support conditions. Complete poles are formed around the wall extremities, achieving a reduction of 28%, just 10% less efficient than the non-modular stress pattern.

Table 1. Performance results, with elastic energy and estimated computation time per design.

	Grid	**Heuristic** Support conditions	**Heuristic** Stress field	**Optimized** Evolutionary algorithm	**Optimized** Simulated annealing	**Manual**	**Stress pattern**
Structural mass [t]	11.4	11.4	11.4	11.4	11.4	11.4	11.4
Rib depth [cm]	20.0	20.0	20.0	20.0	20.0	20.0	20.0
Rib width [cm]	10.0	9.1	8.3	7.8	8.4	8.8	6.2
Elastic energy [kN.m]	0.990	0.779	0.784	0.743	0.726	0.710	0.648
Computation time	0	< 1 s	< 20 s	10 min	10 min	-	-

4.3. Multiple load case analysis

Designs optimized for a single load case are sensitive to the variety of loading scenarios that building floors experience. Based on influence areas, the floor is divided into two areas for asymmetrical loading Q' and Q'' of 5 kN/m^2, shown in Figure 7. The previously found designs are analysed for the two load combinations $G + Q'$ and $G + Q''$ as well, and their robustness against multiple load cases compared using their elastic energy. The numerical results are reported in Table 2, with the same color gradient as in Table 1 per load combination. The best modular design outperforms the non-modular stress pattern for the load combinations with asymmetrical load cases, by 18% for $G + Q'$ and by 1% for $G + Q''$.

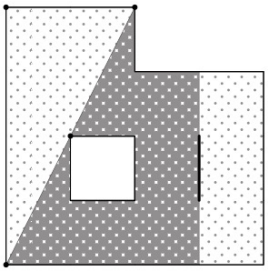

Figure 7. Influence areas for two asymmetrical load cases: Q' in grey and Q'' in white.

Table 2. Performance results under a variety of load cases.

Elastic energy [kN.m]	**Grid**	**Heuristic** Support conditions	**Heuristic** Stress field	**Optimized** Evolutionary algorithm	**Optimized** Simulated annealing	**Manual**	**Stress pattern**
$G + Q$	0.990	0.779	0.784	0.743	0.726	0.71	0.648
$G + Q'$	0.598	0.524	0.558	0.537	0.527	0.499	0.588
$G + Q''$	0.691	0.596	0.592	0.596	0.572	0.571	0.579

4.4. Discussion

The proposed catalogue of 6 modules exhibits performance gains of 20-30% compared to a single-module system, depending on the search method used. Fast heuristic methods, though not the best, yielded efficient designs faster than the optimization methods, without major loss. The heuristic methods can be scaled to problems with a larger configuration space, unlike the optimization methods, which would require significant computation effort. The presented results show the strength of structural design judgement, but they also show that more efficient designs, like the manual one, have been missed by the optimization methods, and that more suitable algorithms may offer a better contribution. Especially considering that multiple load cases, non-quad patterns, coarse discrete structures, and weaker reversible joints, as well as the integration of additional project requirements will challenge heuristics, experience, and judgement to find trade-offs in multi-objective design problems. All these imperfections make an optimized non-modular stress pattern less relevant, as shown when considering asymmetrical load cases, where a modular design is the best performing one. This poly-module design, the manual one, is rendered in Figure 8 to illustrate the proposed modular rib pattern for this case study.

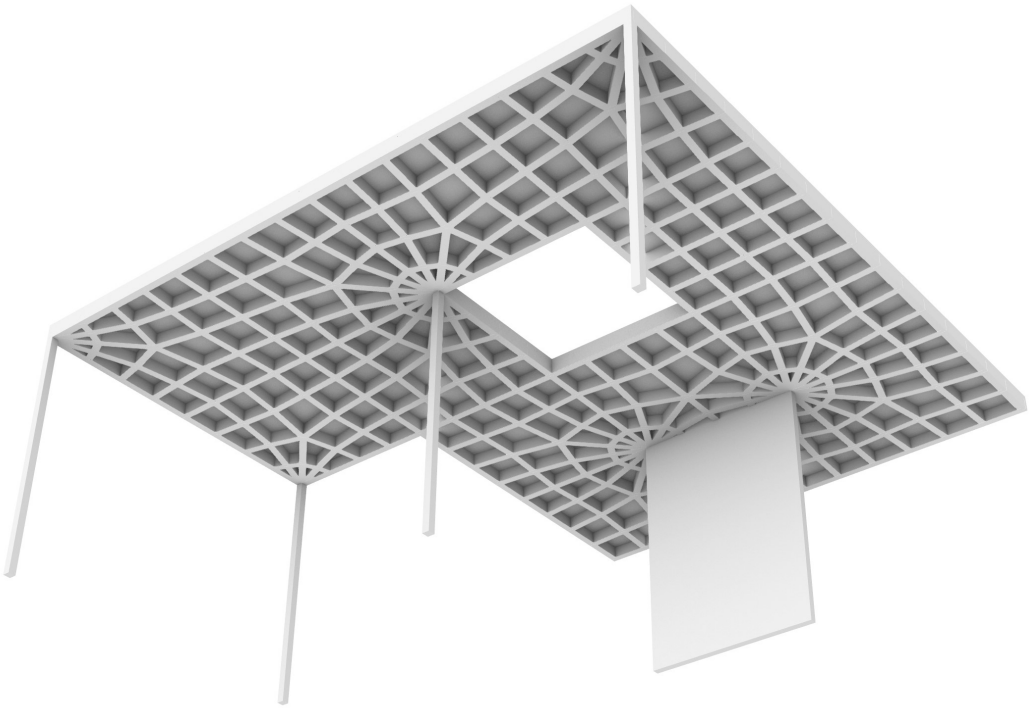

Figure 8. Modular ribbed floor, using three unique modules from a six-module catalogue. This design is 28% more efficient than the grid of a waffle floor and 10% less efficient than a non-modular stress pattern in terms of elastic energy for a uniform live load. This poly-module design outperforms the stress pattern for asymmetrical load patterns. The modules seams are not rendered nor materialized.

5. Conclusion

Poly-modular ribbed building floors offer a trade-off between efficiency, buildability, and circularity. This paper presented a six-module catalogue applied to a case study for which a design configuration could be found that was 28% more efficient than the grid of a waffle floor and only 10% less efficient than a non-modular stress pattern in terms of elastic energy for a uniform loading. However, studying multiple load cases showed that an efficient modular design can outperform a design optimized for a single load scenario when considering multiple structural (and potentially non-structural) objectives. The catalogue can be optimized, and the configuration search enhanced. A series of benchmark building layouts is needed to inform the design of the catalogue, with more realistic structural models, including deflection and stress checks, and weaker reversible joint interfaces. The materialization of this system, particularly the development of reversible bending-resistant joints to allow for dis/re-assembly, as well as the material and element production strategy, will also be essential.

References

[1] P. L. Nervi, C. Chiorino, E. Margiotta Nervi, and T. Leslie, *Aesthetics and technology in building*. University of Illinois Press, Urbana, 2018.

[2] H.-D. Hecker, "Der Hoersaal des Zoologischen Instituts der Universitaet Freiburg", *Freiburger Universitaetsblaetter*, 25:49–52, 1969.

[3] Holedeck, *La estructura de hormigón más sostenible del mundo*, https://holedeck.com, 2024.

[4] G. Pólya, and R.C. Read, *Combinatorial enumeration of groups, graphs, and chemical compounds*. Springer Science & Business Media, 2012.

[5] R. Oval, M. Rippmann, R. Mesnil, T. Van Mele, O. Baverel, and P. Block, "Feature-based topology finding of patterns for shell structures", *Automation in Construction*, 103:185-201, 2019.

[6] D. Rutten, "Galapagos: On the logic and limitations of generic solvers", *Architectural Design*, 83(2), 132-135, 2013.

[7] C. Preisinger, and M. Heimrath, "Karamba—A toolkit for parametric structural design", *Structural Engineering International*, 24(2):217-21, 2014.